ADVANCED MATERIALS INTERFACES
www.advmatinterfaces.de

Ultrathin-Walled 3D Inorganic Nanostructured Networks Templated from Cross-Linked Cellulose Nanocrystal Aerogels

*Arto Hiltunen, Tyler Or, Kimmo Lahtonen, Harri Ali-Löytty, Nikolai Tkachenko, Mika Valden, Essi Sarlin, Emily D. Cranston, Jose M. Moran-Mirabal, and Jaana Vapaavuori**

A key challenge in the development of materials for applications in the fields of opto- and nanoelectronics, catalysis, separation, and energy conversion is the ability to fabricate 3D inorganic semiconductive nanostructures in a precisely-controlled and cost-effective manner. This work describes the fabrication of 3D nanostructured TiO_2 monoliths by coating ultraporous cross-linked cellulose nanocrystal (CNC) aerogel templates with TiO_2 layers of controlled thickness via atomic layer deposition (ALD). Following calcination, the resulting hollow inorganic ultraporous 3D networks form the thinnest self-supporting semiconductive structure (7 nm) fabricated directly on a conductive substrate. The CNC-templated ALD–TiO_2 electrodes are applied toward photoelectrochemical water splitting. The results show that a TiO_2 coating as thin as 15 nm produces a maximum water splitting efficiency, resulting in materials savings and reduced fabrication time.

1. Introduction

High surface area semiconductors have multiple applications in electronics and energy conversion.[1,2] While conventional photovoltaic devices convert sunlight directly into electricity, photoelectrochemical (PEC) water splitting provides an alternative route to harness this renewable energy source. In PEC cells, water is decomposed at the catalytic metal oxide interface, storing chemical energy in the form of H_2(g). An ideal PEC cell would have a large catalytic surface area, direct electron transport pathways, and optimal sunlight collection.[3] Porous nanostructured semiconductors meet these requirements by increasing the amount of absorbing material and light scattering within the device.[4] However, the fabrication of mesoporous inorganic 3D networks with control over geometry and internal morphology remains a challenge.

In contrast to traditionally used wet synthetic routes, atomic layer deposition (ALD) is a simple coating approach widely applied in modern electronics. In ALD, alternating reactants are deposited onto a substrate, limiting the reaction to its surface layer. Hence, ALD enables deposition of thin films with ultrahigh precision. Ideally, films as thin as one molecular monolayer per ALD cycle can be prepared, and typically the film growth per cycle ranges between 0.01 and 0.3 nm.[5] Thicker layers can be prepared with the same precision by simply increasing the number of ALD cycles, at the expense of longer deposition times.

Cellulose-based materials are attractive as ALD templates due to the variety of structures and surface chemistries available. Kemell et al. were the first to demonstrate templating of TiO_2 by ALD on cellulose filter paper for photocatalysis applications.[6] Hyde et al. characterized ALD coatings on cotton patches, applying Al_2O_3 coatings to tailor the wettability, and $TiNO_x$ coatings to promote cell adhesion and growth.[7,8] For applications requiring porosity and high specific surface area, nanocellulose aerogels provide a template with a hierarchically porous structure, where the average pore size can be controlled in the nanometer to micrometer range.[9,10] For instance, Korhonen et al. coated cellulose nanofibril (CNF) aerogels with TiO_2 and demonstrated their application as humidity sensors and oil absorbents.[11] More recently, Li et al. used CNF aerogels as ALD templates for TiO_2 to prepare capillary photoanodes for water splitting cells.[3] The electrodes wetted with capillary

Dr. A. Hiltunen, Prof. N. Tkachenko
Faculty of Engineering and Natural Sciences
Tampere University
P.O. Box 541, Tampere 33101, Finland
T. Or, Prof. J. M. Moran-Mirabal
Department of Chemistry and Chemical Biology
McMaster University
1280 Main St. West, Hamilton, ON L8S 4M1, Canada
Dr. K. Lahtonen, Dr. H. Ali-Löytty, Prof. M. Valden
Surface Science Group
Laboratory of Photonics
Tampere University of Technology
P.O. Box 692, Tampere FI-33101, Finland
Prof. E. Sarlin
Department of Materials Science
Tampere University of Technology
P.O. Box 589, Tampere 33101, Finland
Prof. E. D. Cranston
Department of Wood Science
University of British Columbia
2424 Main Mall, Vancouver, BC V6T 1Z4, Canada
Prof. E. D. Cranston
Department of Chemical and Biological Engineering
The University of British Columbia
2360 East Mall, Vancouver, BC V6T 1Z3, Canada
Prof. J. Vapaavuori
Department of Chemistry and Materials Science
School of Chemical Engineering
Aalto University
Aalto FI-00076, Finland
E-mail: jaana.vapaavuori@aalto.fi
The ORCID identification number(s) for the author(s) of this article can be found under https://doi.org/10.1002/admi.202001181.

DOI: 10.1002/admi.202001181

action had a higher performance compared to photoanodes completely immersed in the electrolyte.[3] Buesch et al. used ALD to deposit Al_2O_3 on cellulose nanocrystals (CNCs, a rigid, shorter, rod-like form of nanocellulose compared to flexible fiber-like CNF), as a method to increase the contrast of organic nanoscale structures in electron microscopy imaging.[12] In previous work, we have used porous cellulose acetate films as templates to prepare transferable ALD–TiO_2 semiconductive structures.[13,14] However, to the best of knowledge, all prior studies have either focused on using bulk cellulosic materials as templates or investigated only one ALD coating thickness. To expand the range of applications for ALD-templated semiconductive structures, it is important to develop approaches where the porosity and physical dimensions of the template can be controlled precisely and fabricated directly on conductive substrates.

Aerogels made out of CNCs meet the requirements of simple fabrication and structural customization, due to the versatility of the CNC surface chemistry, the control over the dry cellulose content, and the possibility to vary the shape, thickness, density, and porosity of the aerogel patterns. In addition, CNC aerogels can be prepared with milder processing conditions compared to CNF aerogels.[15,16] Due to their thermal and chemical stability, as well as their ability to form liquid crystals, CNCs have been used as morphology-inducing templates for different types of mesoporous titania structures.[17–20] In this work, we employ tailored CNC aerogel templates[15,21] fabricated on conductive fluorine-doped tin oxide (FTO)-coated glass substrates to produce porous nanostructured TiO_2 electrodes.

Since the aerogel film fabrication method used in this work allows control over film thickness and density,[15] we optimized the aerogel template thickness to enable the uniform diffusion of ALD precursors. The precursors reacted to form TiO_2 coatings and the aerogel template was subsequently calcined, resulting in a mesoporous and continuous TiO_2 network in direct contact with the conductive substrate. In this way, we were able to transform 10 µm thick CNC aerogel templates into hollow nanoporous and mechanically stable networks composed of ALD–TiO_2 fibers with walls that were as thin as 7 nm. When the coating was 15 nm thick, 100% improvement in solar water splitting efficiency over a planar device was obtained, clearly demonstrating the vast possibilities for optimization with respect to device performance and material consumption.

2. Results and Discussion

Cross-linked cellulose nanocrystal aerogel templates with controllable dimensions were fabricated using a recently developed pressure-aided freeze casting technique.[15] Briefly, aqueous suspensions of aldehyde- and hydrazide-functionalized CNCs were mixed and this mixture was cast on a transparent conducting substrate masked by an adhesive stencil film. Next, the sample was capped with an aluminum dish and pressure was applied for the aqueous mixture to fill the stencil opening. The suspension was subsequently frozen to promote the formation of hydrazone cross-links between the orthogonally-functionalized CNCs and lyophilized to remove the ice from within the CNC network.[22] Finally, the stencil was peeled off to reveal the patterned aerogel film on the substrate. The CNC aerogels used in this work have been thoroughly characterized in an earlier work. The specific surface area of the aerogels was reported to be above 200 $m^2\ g^{-1}$.[22]

To convert the CNC aerogel films into 3D structured porous inorganic electrodes, the films were placed in the ALD chamber without further processing. Owing to the good thermal stability of the CNC films,[23] a tetrakis(dimethylamino)titanium/H_2O ALD cycle at 200 °C could be used for the deposition of TiO_2. According to thermogravimetric analysis, the onset of degradation of aldehyde-functionalized CNC (one of the two precursors of the aerogels) was observed below the TiO_2 deposition temperature, however, the maximum rate of degradation of both CNC precursors occurs above 250 °C enabling the deposition at 200 °C (see Figure S1 for the TGA graphs, Supporting Information). Upon deposition the films were amorphous with some Ti^{3+} defects[24] that led to a dark appearance (**Figure 1**).[25] The films were then calcined in air at 500 °C, which induced a color change to white due to the oxidation of Ti^{3+} traces and crystallization of amorphous TiO_2.[26]

To optimize the diffusion of the gaseous TiO_2 precursors into the cellulose aerogel network, two different aerogel densities were investigated. The aerogel density was effectively tuned by changing the concentration of the CNC suspension (containing equal mass ratio of aldehyde- and hydrazide-functionalized CNCs) used during freeze-casting from 1 to 2.5 wt%. At 2.5 wt%, we observed that some of the pores were blocked due to the accumulation of material in thicker ALD–TiO_2 coatings. Therefore, 1 wt% CNC suspensions were used in all subsequent experiments to ensure that maximum porosity was retained. Scanning electron microscopy (SEM)

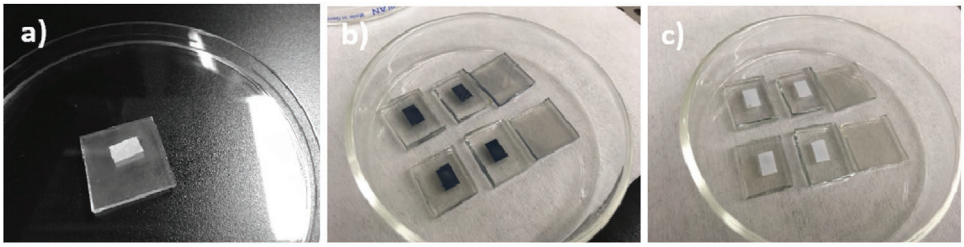

Figure 1. Photographs of films at different stages of fabrication. a) CNC aerogel template on FTO glass, b) films after ALD deposition, c) films after calcination. The samples on the right, in (b) and (c) are FTO substrates having the equivalent amount of ALD–TiO_2 (145 cycles, 7 nm) deposited on them as on the CNC aerogels. The substrate size is 2×2 cm^2.

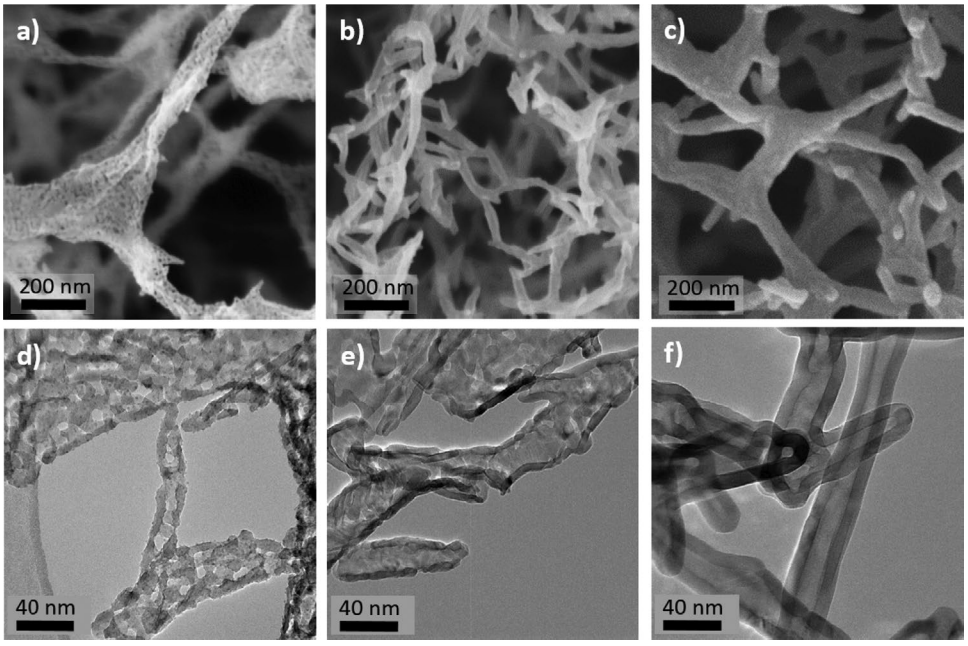

Figure 2. a–c) SEM and d–f) transmission electron microscopy (TEM) images of the cellulose-templated ALD–TiO_2 networks (87, 145, 290 ALD-cycles) after calcination. The CNC aerogel films were cast from 1 wt% suspension.

images comparing films cast from 1 and 2.5 wt% suspensions are provided in Figure S2 (Supporting Information). Aerogels produced from 1 wt% CNC suspensions resulted in porous hollow branching network structures that were in direct contact with the underlying substrate. Once this optimal aerogel composition was found, ALD-deposited TiO_2 coatings with different thicknesses were investigated, starting from 30 nm (the thinnest reported functional coating obtained by using sacrificial cellulose templates)[3,13] down to a thickness (a patchy coating < 5 nm) that did not produce a self-supporting structure.

The CNC aerogel templates were mechanically stable and able to withstand all of the tested ALD–TiO_2 deposition conditions and cycles, resulting in self-supporting ALD–TiO_2 coated aerogels. However, once the CNC aerogel template was removed via calcination (at 500 °C), the ALD–TiO_2 structure would collapse if the coating was too thin. The structures that had 87 cycles or thicker TiO_2 coating were stable after annealing and tolerated normal handling well. **Figure 2** shows SEM and transmission electron microscopy (TEM) images of self-supporting TiO_2 aerogels after template removal. ALD–TiO_2 coatings were deposited using 87 (nominal thickness of 3.0 nm), 145 (5.0 nm), and 290 (10.0 nm) cycles. The resulting film thicknesses were 7 ± 2, 7 ± 2, 11 ± 1 nm, respectively, as measured from the TEM images (Figure 2). The coating thickness was uniform throughout the film. In our previous work,[27] the coating thickness was found to decrease toward the bottom of the film due to limited diffusion of ALD precursors within the comparatively more dense cellulose acetate template. This issue was resolved using the more porous CNC aerogel templates (see Figure S3 (Supporting Information) for SEM images from the top and bottom of the films). Attempts to reduce the number of deposition cycles resulted in collapse of the structure during calcination (Figure S4, Supporting Information). The reason for the collapse after calcination was the nonconformal TiO_2 coverage of the aerogel occurring in the early stage of the film growth that left holes in the ALD–TiO_2 coating. The holes can be clearly observed in the SEM and TEM images of a coating deposited using 87 ALD cycles (Figure 2a,d), but are not apparent after 145 cycles (Figure 2b,e). Thus, in the early stages of the coating, the TiO_2 accumulated in a nonhomogeneous fashion, and then later cycles eventually filled the holes. Similar nonconformal film growth at low cycle numbers has been previously reported for the ALD–TiO_2 coating of carbon nanotubes.[28]

To date, all the reported ALD and chemical vapor deposition (CVD) coating thickness values with processes requiring template removal have been on the order of tens of nanometers, as shown in **Table 1**. In this work, we report a standing 3D network with 7 nm coating thickness that is, to the best of our knowledge, the thinnest self-supporting structure fabricated by means of template removal (**Figure 3**). Previously, Kettunen et al. achieved a 7 nm coating thickness without template removal with only one CVD cycle that consisted of a 2 h long titanium isopropoxide treatment step and a 2 h long N_2 purging step.[29] While the use of long reaction times is justified to ensure complete coverage of the porous template, it is impractical for thicker coatings that require multiple cycles. With our method, the same 7 nm coating thickness was reached in ≈15 min, making it thus much faster than the previously reported CVD method. Furthermore, many intermediate coating thicknesses could easily be prepared due to the higher adjustability of ALD as compared to CVD.

To demonstrate that the high tunability of aerogel templates combined with ALD allow for systematic device optimization, we first optimized the thickness of the aerogel templates[15] and then applied the prepared TiO_2 networks as porous hyperbranched photoanodes for PEC cells. By adjusting the

Table 1. Comparison of ALD or CVD (chemical vapor deposition) prepared coating thicknesses on cellulose templates.

Template	Material	Method	Cycles	Coating thickness	Template removal	Reference
CNCs	TiO_2	ALD	87–870	7–30 nm	Yes	Reported here
CNFs	TiO_2	CVD	1	7 nm	No	[28]
Woven cotton	Al_2O_3	ALD	1–200	up to 22 nm	No[a)]	[7]
CNFs	TiO_2, ZnO, Al_2O_3	ALD	50–300	N/A	Yes	[11]
Filter paper	TiO_2	ALD	1000	30–55 nm	Yes	[6]
Cellulose acetate	TiO_2	ALD	480	30 nm	Yes	[13]
CNFs	TiO_2	ALD	350[b)]	30 nm	Yes	[3]
CNCs	Al_2O_3	ALD	80	20	No	[2]

[a)]Template removal reported for 700 cycles coating; [b)]Additional 400 cycles were applied to complete the electrode.

number of the ALD cycles, the impact of the coating thickness on the efficiency of the PEC water splitting was investigated. **Figure 4**a shows *I–V* curves of devices with varying ALD–TiO_2 coating thickness. It was observed that the electrodes prepared with 435 cycles (15 nm) of TiO_2 resulted in similar photocurrent values as the ones prepared with 870 cycles (30 nm), while only requiring half the coating material. This is significant, when anticipating the large-scale production of porous semiconductive structures. Figure 4b compares the photocurrent achieved with the hierarchically branched porous TiO_2 electrode to a planar TiO_2 coating on a bare FTO-glass. Using a coating thickness of 15 nm, the porous 3D network resulted in a doubling of the photocurrent values, showcasing the benefits of the 3D branched networks over planar devices.

Compared to planar cells, the use of CNC-based aerogels for templating has advantages in water splitting cells due to their hierarchically porous structure. Macropores provide low-resistance pathways for water to diffuse through the porous network, while mesopores enhance the catalytic surface area. Moreover, using porous templates makes it possible to achieve high optical absorbance with extremely thin coatings that would otherwise be transparent on planar surfaces. As compared to the CNF aerogels used by Li et al.,[3] our system based on aldehyde-hydrazide (i.e., hydrazone) cross-linked CNCs is easier to tune, since the porosity of the aerogel networks can be modulated by varying the concentration of the cross-linking components in the suspension before lyophilization. The much milder freezing conditions as compared to the flash-freezing or supercritical drying required for CNF aerogels[10] are suitable to produce a plethora of 3D network architectures. Taken into account that cellulose is the most abundant polymer on the Earth,[30] CNCs are ideal template materials in addition to being safe to handle and produce.[31,32]

3. Conclusion

In this work, the fabrication of ultraporous monolithic nanostructured TiO_2 networks was achieved, for the first time, through the combination of CNC aerogel templating and TiO_2 ALD deposition. This strategy allowed optimizing the dimensions and porosity of the monolith, to achieve uniform ALD deposition, as well as the minimum thickness of the TiO_2 coatings to maintain the structural integrity of the 3D network after the CNC template was removed. Experiments performed at a very small number of coating cycles revealed the early stages of ALD–TiO_2 film growth, which began as the deposition of weakly connected crystallites that eventually fused together creating a conformal layer on the surface. At the limit of mechanical stability, self-standing uniform 7 nm thick ALD–TiO_2 coatings could replicate the shape of the porous branching aerogel network. Our strategy allowed for the direct fabrication of a semiconductive photoelectrode, because all of the processing could be done directly on a transparent conductive substrate.

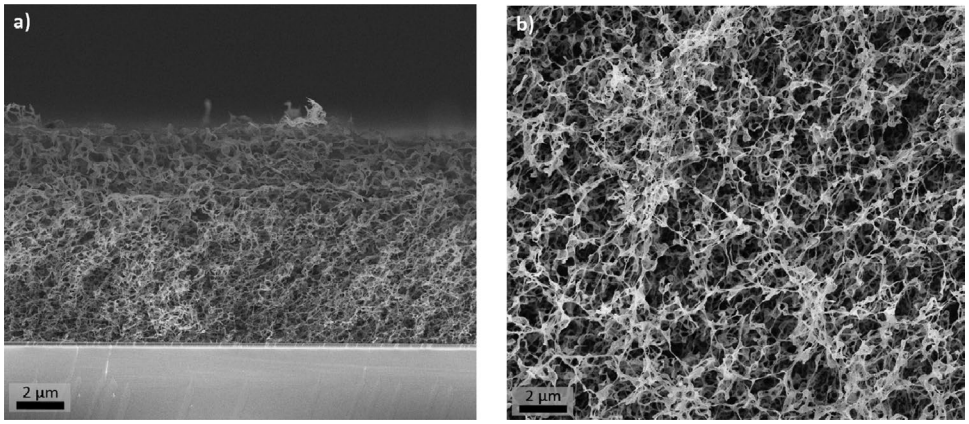

Figure 3. SEM image of the thinnest self-supporting ALD–TiO_2 aerogel (87 cycles = 7 nm, annealed). a) Cross-section, b) imaged from the top.

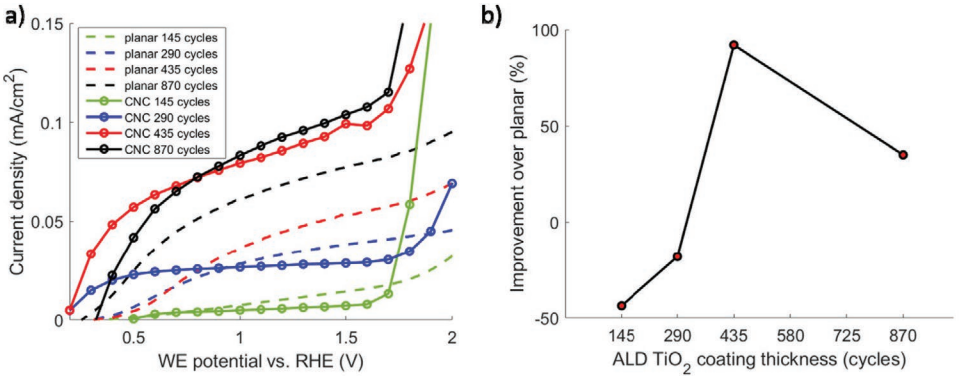

Figure 4. a) *I–V* curves of the CNC templated TiO_2 3D structures compared with planar samples having the same TiO_2 coating thickness (870 cycles; 30 nm, 435 cycles; 15 nm, 290 cycles; 10 nm, 145 cycles; 5 nm). b) Improvement on the photocurrent at 1.23 V versus RHE achieved using CNC templates relative to planar samples with same coating thickness.

Moreover, TiO_2 layer thickness in photoelectrochemical water splitting cells was optimized, thus reducing raw materials consumption while maximizing energy production. These results showcase the vast potential of cellulose templating combined with atomic layer deposition in a broad range of applications in the fields of optics, catalysis, and nanoelectronics.

4. Experimental Section

CNC Template Fabrication: Sulfate half-ester functionalized CNCs (sCNCs) were produced by hydrolyzing ashless cotton filter aid (Whatman, GE Healthcare Life Sciences, CAT No. 1703-050, Mississauga, Canada) in 64 wt% sulfuric acid (Caledon Laboratories, Mississauga, Canada).[33] The sCNCs were functionalized with aldehyde groups (aCNCs) using a sodium periodate (Sigma-Aldrich, Oakville, Canada) oxidation route as described in prior work.[34] The aCNCs generated had a z-average mean particle size of 92 ± 8 nm determined by dynamic light scattering (Malvern Zetasizer 3000, Malvern, UK, assuming spherical particle shape in the calculation and thus only used for relative comparison of size and to show good particle dispersion), zeta potential of −16 ± 2 mV (ZetaPlus Zeta Potential Analyzer, Brookhaven Instruments, Holtsville, NY), and an aldehyde functionalization content of 1.56 ± 0.09 mmol g^{-1} as determined by conductometric titration (VWR sympHony). Hydrazide functionalized CNCs (hCNCs) were produced as described previously[34] by first oxidizing sCNCs with 2,2,6,6-tetramethyl-1-piperidinyloxy (TEMPO, Sigma-Aldrich). The resulting carboxyl groups on the CNCs were activated using *N*′-ethyl-*N*-(3-(dimethylamino)propyl)-carbodiimide (EDC, Sigma-Aldrich) and *N*-hydroxysuccinimide (NHS, Sigma-Aldrich), then reacted with adipic acid dihydrazide (ADH, Sigma-Aldrich). The hCNCs had a z-average mean particle size of 108 ± 1 nm, zeta potential of −36 ± 5 mV, and a hydrazide functionalization content of 0.50 ± 0.07 mmol g^{-1}.

Aerogel films (1 or 2.5 wt% sol–gel concentration, 1:1 aCNC:hCNC weight ratio) were patterned onto FTO-coated glass (TEC-15, Pilkington, UK, sheet resistance 15 Ω sq^{-1}) substrates using a recently developed pressure-aided freeze casting technique. Briefly, FTO-coated glass was cleaned with Piranha solution (5:1 H_2SO_4: H_2O_2 v/v) for 15 min at 110 °C to remove organic residue. A 7 µm thick Parylene (Specialty Coating Systems, Indianapolis, IN) film was deposited on the counter-electrode and the film was patterned by xurography to create 5 × 8 mm molds. It should be noted that prior to Parylene deposition the substrate was spin-coated with surfactant (1% v/v, Micro-90, International Products Corp., Burlington, NJ) to reduce the adhesion of the Parylene. To ensure no interference with gel casting, the surfactant was washed from the substrate by bath sonication in water for 15 min. Premixed aCNC:hCNC sol–gel suspensions were drop-cast on the mold and immediately frozen at −30 °C, while under pressure. The frozen gel was lyophilized and the mold was subsequently lifted-off to reveal the aerogel of desired thickness and pattern.

Atomic Layer Deposition: The amorphous black titanium oxide thin film was grown on the CNC templates by ALD using $Ti(N(CH_3)_2)_4/H_2O$ process at 200 °C in a Picosun Sunale R-200 Advanced reactor. The average growth per cycle of 0.0345 nm was determined on a native oxide of a n-Si(100)(P) wafer by Rudolph Research Analytical Auto EL III ellipsometer.

Calcination: After the ALD the samples were calcined in air at 500 °C for 1 h using a heating rate of 20 °C min^{-1}. Samples were cooled down slowly inside the oven to room temperature.

Photoelectrochemical Characterization: The photoelectrochemical tests were performed using a 3-electrode setup having the sample as the working electrode, a plating counter electrode and Ag/AgCl (3 M NaCl) as the reference electrode. Electrolyte was 0.1 M NaOH contained in a 1 × 5 cm quartz cuvette. The samples were illuminated through the substrate using a AAA-class solar simulator (Sciencetech SS150-AAA) adjusted to 100 mW cm^{-2} (1 Sun) light intensity. Typical photoelectrode size was 50 mm^2 square, and rest of the substrate was isolated from the reaction using tape.

SEM: For cross sectional SEM images the samples were cut in half using a glass cutter pen. The images were taken with a field emission scanning electron microscope (FESEM) Carl Zeiss Ultra 55 instrument. Typical acceleration voltage was 3 kV.

TEM: Jeol TEM 2010 was used to study individual TiO_2 tubes. A small amount of the ALD–TiO_2 network was scraped to ethanol. A droplet of the ethanol was then placed on a TEM copper grid with a hollow carbon film. After evaporation of ethanol at room temperature, the samples where studied with an acceleration voltage of 200 kV.

Thermogravimetric Analysis (TGA): Analyses were carried out on a TA Instruments Q50 thermogravimetric analyzer. Data were collected after placing ≈10 mg of a vacuum-dried sample in a clean platinum pan and heating from ambient temperature to 800 °C under argon atmosphere (heating rate of 20 °C min^{-1}).

Supporting Information

Supporting Information is available from the Wiley Online Library or from the author.

Acknowledgements

All the co-authors acknowledge Dr. Ayodele Fatona with gratitude for the assistance with TGA measurements. This work was supported by the Academy of Finland (Decision Nos. 141481, 286713, and 309920). T.O.

was partially supported through a Natural Sciences and Engineering Research Council of Canada Undergraduate Student Research Award (NSERC-USRA). J.M.M. and E.D.C. are recipients of Early Researcher Awards from the Ontario Ministry of Research and Innovation and J.M.M. holds the Tier 2 Canada Research Chair in Micro- and Nanostructured Materials. Funding from NSERC through Discovery Grants to J.M.M. and E.D.C. is gratefully acknowledged. This research made use of instrumentation in the Canadian Centre for Electron Microscopy and Biointerfaces Institute at McMaster University. This work is part of the Academy of Finland Flagship Programme, Photonics Research, and Innovation (PREIN) (Decision No. 320 165).

Conflict of Interest

The authors declare no conflict of interest.

Data Availability Statement

Research data are not shared.

Keywords

3D network structure, atomic layer deposition, nanocellulose, templating, water splitting

Received: July 3, 2020
Revised: March 24, 2021
Published online: May 7, 2021

[1] K. Lee, A. Mazare, P. Schmuki, *Chem. Rev.* **2014**, *114*, 9385.
[2] D. Fattakhova-Rohlfing, A. Zaleska, T. Bein, *Chem. Rev.* **2014**, *114*, 9487.
[3] Z. Li, C. Yao, Y. Yu, Z. Cai, X. Wang, *Adv. Mater.* **2014**, *26*, 2262.
[4] M. J. Bierman, S. Jin, *Energy Environ. Sci.* **2009**, *2*, 1050.
[5] M. Leskelä, M. Ritala, *Angew. Chem., Int. Ed.* **2003**, *42*, 5548.
[6] M. Kemell, V. Pore, M. Ritala, M. Leskelä, M. Lindén, *J. Am. Chem. Soc.* **2005**, *127*, 14178.
[7] G. K. Hyde, G. Scarel, J. C. Spagnola, Q. Peng, K. Lee, B. Gong, K. G. Roberts, K. M. Roth, C. A. Hanson, C. K. Devine, S. M. Stewart, D. Hojo, J. S. Na, J. S. Jur, G. N. Parsons, *Langmuir* **2010**, *26*, 2550.
[8] G. K. Hyde, S. D. McCullen, S. Jeon, S. M. Stewart, H. Jeon, E. G. Loboa, G. N. Parsons, *Biomed. Mater.* **2009**, *4*, 025001.
[9] Y. K. Akimov, *Instrum. Exp. Tech.* **2003**, *46*, 287.
[10] K. J. De France, T. Hoare, E. D. Cranston, *Chem. Mater.* **2017**, *29*, 4609.
[11] J. T. Korhonen, P. Hiekkataipale, J. Malm, M. Karppinen, O. Ikkala, R. H. A. Ras, *ACS Nano* **2011**, *5*, 1967.
[12] C. Buesch, S. W. Smith, P. Eschbach, J. F. Conley, J. Simonsen, *Biomacromolecules* **2016**, *17*, 2956.
[13] A. Hiltunen, K. Lahtonen, J. Saari, A. Ojanperä, E. Sarlin, H. Wondraczek, A. Efimov, K. Kaunisto, P. Vivo, C. Maccato, D. Barreca, P. Fardim, N. Tkachenko, M. Valden, H. Lemmetyinen, *ChemPhysChem* **2017**, *18*, 64.
[14] A. Hiltunen, T. P. Ruoko, T. Iivonen, K. Lahtonen, H. Ali-Löytty, E. Sarlin, M. Valden, M. Leskelä, N. Tkachenko, *Sustainable Energy Fuels* **2018**, *2*, 2124.
[15] T. Or, S. Saem, A. Esteve, D. A. Osorio, K. J. De France, J. Vapaavuori, T. Hoare, A. Cerf, E. D. Cranston, J. M. Moran-Mirabal, *ACS Appl. Nano Mater.* **2019**, *2*, 4169.
[16] Y. Habibi, *Chem. Soc. Rev.* **2014**, *43*, 1519.
[17] A. Ivanova, D. Fattakhova-Rohlfing, B. E. Kayaalp, J. Rathouský, T. Bein, *J. Am. Chem. Soc.* **2014**, *136*, 5930.
[18] X. Chen, D. H. Kuo, D. Lu, *Chem. Eng. J.* **2016**, *295*, 192.
[19] Y. Zhou, E. Y. Ding, W. D. Li, *Mater. Lett.* **2007**, *61*, 5050.
[20] K. E. Shopsowitz, A. Stahl, W. Y. Hamad, M. J. MacLachlan, *Angew. Chem., Int. Ed.* **2012**, *51*, 6886.
[21] T. Or, K. Miettunen, E. D. Cranston, J. M. Moran-Mirabal, J. Vapaavuori, *ACS Appl. Energy Mater.* **2019**, *2*, 5635.
[22] X. Yang, E. D. Cranston, *Chem. Mater.* **2014**, *26*, 6016.
[23] M. Roman, W. T. Winter, *Biomacromolecules* **2004**, *5*, 1671.
[24] M. Hannula, H. Ali-Löytty, K. Lahtonen, E. Sarlin, J. Saari, M. Valden, *Chem. Mater.* **2018**, *30*, 1199.
[25] B. Wang, S. Shen, S. S. Mao, *J. Mater.* **2017**, *3*, 96.
[26] H. Ali-Löytty, M. Hannula, J. Saari, L. Palmolahti, B. D. Bhuskute, R. Ulkuniemi, T. Nyyssönen, K. Lahtonen, M. Valden, *ACS Appl. Mater. Interfaces* **2019**, *11*, 2758.
[27] A. Hiltunen, K. Lahtonen, J. Saari, A. Ojanperä, E. Sarlin, H. Wondraczek, A. Efimov, K. Kaunisto, P. Vivo, C. Maccato, D. Barreca, P. Fardim, N. Tkachenko, M. Valden, H. Lemmetyinen, *ChemPhysChem* **2017**, *18*, 64.
[28] Y. Zhang, C. Guerra-Nuñez, I. Utke, J. Michler, M. D. Rossell, R. Erni, *J. Phys. Chem. C* **2015**, *119*, 3379.
[29] M. Kettunen, R. J. Silvennoinen, N. Houbenov, A. Nykänen, J. Ruokolainen, J. Sainio, V. Pore, M. Kemell, M. Ankerfors, T. Lindström, M. Ritala, R. H. A. Ras, O. Ikkala, *Adv. Funct. Mater.* **2011**, *21*, 510.
[30] X. Wang, C. Yao, F. Wang, Z. Li, *Small* **2017**, *13*, 1702240.
[31] T. Kovacs, V. Naish, B. O'Connor, C. Blaise, F. Gagné, L. Hall, V. Trudeau, P. Martel, *Nanotoxicology* **2010**, *4*, 255.
[32] M. Roman, *Ind. Biotechnol.* **2015**, *11*, 25.
[33] S. Beck-Candanedo, M. Roman, D. G. Gray, *Biomacromolecules* **2005**, *6*, 1048.
[34] D. A. Osorio, B. Seifried, P. Moquin, K. Grandfield, E. D. Cranston, *J. Mater. Sci.* **2018**, *53*, 9842.